Czech Technical University in Prague
Faculty of Nuclear Sciences and Physical Engineering
Department of Physics

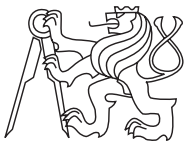

Research thesis

Lukáš Sedlák

Prague 2013

Czech Technical University in Prague
Faculty of Nuclear Sciences and Physical Engineering
Department of Physics

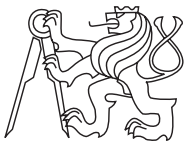

Throughput measurement of multichannel system for visible radiation study on tokamak COMPASS and it's relation calibration

Research thesis

Author: **Lukáš Sedlák**
Leader: **Ing. Diana Naydenkova**
Academic year: **2012/2013**

Statement

I proclaim that I elaborated my research thesis alone and I used basics listed in Bibliography only. (literature, projects, software, etc.)

I have not any reason against the thesis usage *a posteriori* § 60 law number 121/2000 Sb., author's law, laws dependent on author's law and changes some laws (author's law).

In Prague at _____ _____

Lukáš Sedlák

Abstract Fusion power plant requires precise plasma edge control. Disruptions have to be described, predicted and prevented. The plasma edge diagnostics are build on COMPASS tokamak in Prague. New passive multichannel diagnostics in visible light range with time and spatial resolution is in final stage of development.

Keywords: multichannel diagnostics, visible light, time resolution, spatial resolution, plasma, impurities, tokamak, COMPASS

Prologue This paper is intended to be a documentation and partially a textbook to the mentioned diagnostics, rather than a fairy tail about it. Its then only natural that it requires deep understanding of mathematics, plasma physics, spectroscopy, and electronics. Many basic definitions and theorems are included. As it is, it does not include common introductions and small talks which may be found in books or journals. Well-known mathematical schema definition-theorem-proof is used. This schema should ease searching and improve further usage.

Proper documentation should contain blueprints, calibrations and all necessary theory for proper usage of the diagnostics. Unfortunatelly, not all those things are enlisted in this paper. Hopefully, all those things will be enlisted in future version, which may bring name diploma thesis. Thus, the reader should consider this paper as documentation draft with theory background rather than full-scale complete documentation.

Common issue of technical literature is theory depth. Presented theorems require quantity definitions, another theorems or lemmas. Some are included, some are not. In the second case, reader is referred to university textbooks. Some of them are listed in bibliography. Finally, this essential problem may be solved or at least eased in future. Physics theory written by the author in definition-theorem-proof schema is under heavy development.

Contents

Chapter 1

Theory

1.1 Mathematics

1.1.1 Definition

Delta function $\delta(x) : \mathbb{R} \to \mathbb{R}^*$ is defined as

$$\delta(x) \equiv \begin{cases} 0 & x \neq 0 \\ \infty & x = 0 \end{cases}$$

1.1.2 Definition

Heaviside function $\Theta(x) : \mathbb{R} \to \{0, 1\}$ is defined as

$$\Theta(x) \equiv \begin{cases} 0 & x < 0 \\ 1 & x > 0 \end{cases}$$

1.1.3 Theorem

$$\Theta(a) \cdot \Theta(b) = \Theta(\mathsf{min}\{a, b\})$$

Without proof.

1.1.4 Definition

Convolution of functions $f(x), g(x) : \mathbb{R} \to \mathbb{R}$ is defined as

$$f * g(x) \equiv \int_{\mathbb{R}} f(s)g(x - s)ds$$

1.1.5 Definition

Square signal of electric current with power $P_{sq}(t)$ is defined as

$$P_{sq}(t) = A \cdot [\Theta(t - t_0) - \Theta(t - t_1)]$$

where $t_0, t_1 \in \mathbb{R}$ are times of signal start and end, $A \in \mathbb{R}$ is amplitude, see Fig.1.1.5.

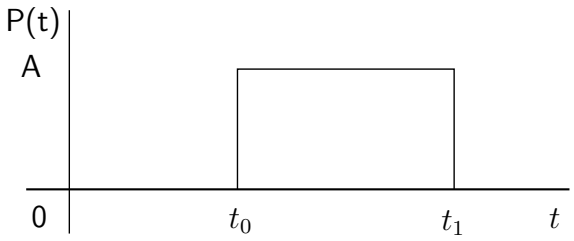

Figure 1.1: Square signal

1.1.6 Theorem

Lets assume infinite conical space based on solid angle Ω with top point $\vec{x}_1$. Lets assume point $\vec{x}_2$ inside the infinite cone. Lets assume maximal radius r of sphere S inside Ω and around point $\vec{x}_2$. Lets assume $r \ll |\vec{x}_2 - \vec{x}_1|$. Then for quantity $q(t, \vec{x}, \vec{k})$

$$\forall \vec{x} \in \Omega \wedge \vec{k} \approx \vec{x}_2 - \vec{x}_1 : \qquad q(t, \vec{x}, \vec{k}) \sim |\vec{x} - \vec{x}_2| \wedge q(t, \vec{x}, \vec{k}) \gg 0$$

$$\forall \vec{x} \in \mathbb{R}^3 - \Omega \vee \vec{k} \not\approx \vec{x}_2 - \vec{x}_1 : \qquad q(t, \vec{x}, \vec{k}) \approx 0$$

exists constant $c \in \mathbb{R}$

$$\iint_{\Omega} q(t, \vec{x}, \vec{k}) d\vec{x} d\vec{k} = c \cdot q(t, \vec{x}_2)$$

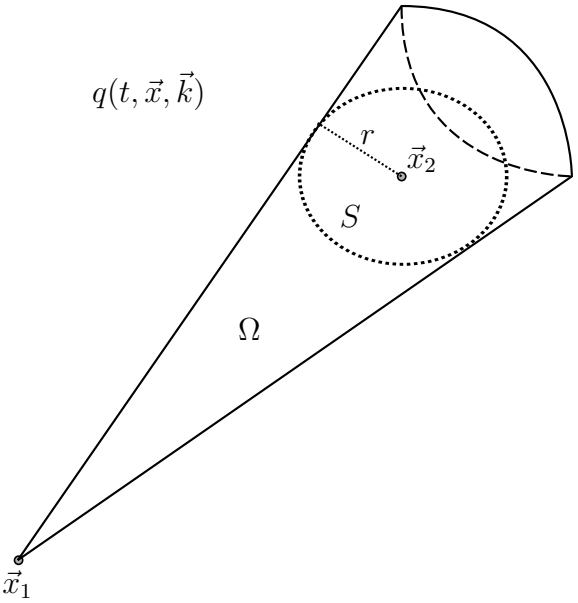

Figure 1.2: Allowed vector approximation schema

Without proof.

1.2 Continuum

1.2.1 Definition

Continuum system $\mathcal{S}_c$ is defined as ordered set of particle density $\rho(t, \vec{x})$, energy density $e(t, \vec{x})$ and volume $\Omega \subset \mathbb{R}^3$

$$\mathcal{S}_c \equiv \{\rho(t, \vec{x}), \Omega\}$$

1.2.2 Definition

Quasineutral continuum system $\mathcal{S}_c$ with i particle types with densities $\rho_i(t, \vec{x})$ and charges z_i is defined as

$$\sum_i z_i \rho_i(t, \vec{x}) = 0$$

1.2.3 Definition

Power $P(t)[W]$ is defined for continuum system $\mathcal{S}_c$ according to SI unit system from total energy $E = \int e(t, \vec{x}) d\Omega dt$ and time t as

$$P(t) \equiv \frac{dE}{dt}$$

1.2.4 Definition

Radiance $L[Wm^{-2}sr^{-1}]$ is defined for continuum system $\mathcal{S}_c$ in SI derived units [9] as

$$L = \frac{dE}{dA \cos \Theta d\Omega dt}$$

where $A[m^2]$ is area, $\Omega[sr]$ solid angle, $\Theta[rad]$ angle between the normal of the surface element dA and the direction of the radiation, see 1.3, [9].

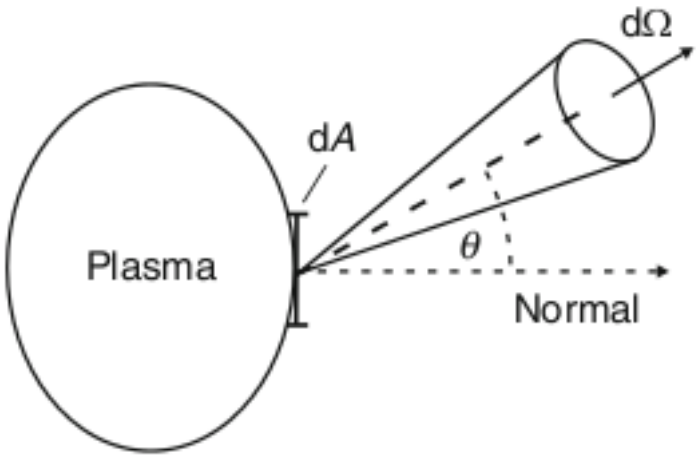

Figure 1.3: Radiance [9]

1.2.5 Theorem

Lets assume radiance L of a light source with area S_p and detector with area S_d. Then for flux P from light source to detector happens [9]

$$P = \iint L \cos\theta \cos\gamma s^{-2} dS_d dS_p$$

Without proof.

1.2.6 Definition

Spectral energy density u_ω is defined [1]

$$u_\omega \equiv \frac{d^2 E}{d\omega d\Omega}$$

where ω frequency, Ω solid angle.

1.2.7 Definition

Intenisty $I(\omega, \Omega)$ is defined (for neglected dispersion) for system with spectral energy density u_ω [1] as

$$I(\omega, \Omega) \equiv c \cdot \frac{du_\omega(\Omega)}{d\Omega}$$

or

$$u_\omega = \frac{1}{c} \int I(\omega, \Omega) d\Omega$$

1.2.8 Definition

Line shape $L(\omega)$ is defined as

$$L(\omega) \equiv \sum_{if\alpha} \delta(\omega - \omega_{if}^s) |\langle f|x_\alpha|i\rangle|^2 \rho_i$$

which meets also

$$\sum |\langle f|x_\alpha|i\rangle|^2 \rho_i = 1$$

It is spectral power emitted by a quantuum mechanical system due to dipole transitions between initial states i and final states f.

1.2.9 Theorem

Lets assume system with spectral power $P(\omega)$ and line shape $L(\omega)$. Then [1]

$$P(\omega) = \frac{4mr_0}{3c} \omega^4 L(\omega)$$

Without proof.

1.2.10 Definition

Line shape operator $\mathcal{L}(\omega)$ is defined for line shape $L(\omega)$ [1]

$$L(\omega) - \frac{\hbar}{\pi}\Im TrD[\hbar\omega - H - \mathcal{L}(\omega)]^{-1}$$

where H hamiltonian of the system.

1.2.11 Definition

Emission coefficient $\varepsilon(\omega, T)$ is defined for radiative loss power density P as [1]

$$P = \iint \varepsilon(\omega, T) d\omega d\Omega$$

where ω frequencies and Ω solid angle.

1.2.12 Theorem

Lets assume continuum system with probability p for a photon to be absorbed and immediately reemited in the line, $R(\omega, \Omega, \omega', \Omega')$ redistribution function alias probability for resonant scattering of photon ω', Ω' into photon ω, Ω, $\kappa_l(\omega)$ line absorption coefficient, $\varepsilon_l(\omega)$ line emission coefficient, $I(\omega', \Omega')$ intensity, $\varepsilon_c(\omega)$ continuum emission coefficient. Then for volume emission coefficient $\varepsilon(\omega, \Omega)$ happens [1]

$$\varepsilon(\omega, \Omega) = p \int \kappa_l(\omega') R(\omega, \Omega, \omega', \Omega') I(\omega', \Omega') d\omega' d\Omega' + (1 - p)\varepsilon_l(\omega) + \varepsilon_c(\omega)$$

Without proof.

1.2.13 Theorem

Lets assume continuum system $\mathcal{S}_c$ with line emission coefficient $\varepsilon_l(\omega)$, line shape $L(\omega)$ and transition probability A_{nm}. Then

$$\varepsilon_l(\omega) = \frac{\hbar\omega}{4\pi} L(\omega) A_{nm} N_m$$

where N_m number of m states.

Without proof.

1.2.14 Theorem

Lets assume system with transition probability A_{nm} and oscillator strength f_{nm}. Then

$$A_{nm} = \frac{2r_0\omega^2}{c} f_{nm}$$

Without proof.

1.2.15 Definition

Line width w is defined for line shape function $\mathcal{L}(\omega)$ as [1]

$$w \equiv -\frac{Im\langle i|\mathcal{L}(\omega_0)|i\rangle}{\hbar}$$

where i is initial state.

1.2.16 Definition

Line shift d is defined for line shape function $\mathcal{L}(\omega)$ as [1]

$$w \equiv -\frac{Re\langle i|\mathcal{L}(\omega_0)|i\rangle}{\hbar}$$

where i is initial state.

1.2.17 Definition

Doppler broadening parameter ω_D is defined for plasma with kinetic temperature T, radiator with mass M and transition frequency ω_0 as

$$\omega_D \equiv \left(\frac{2kT}{Mc^2}\right)^{1/2} \cdot \omega_0$$

1.2.18 Definition

Doppler broadening shape $L_D(\omega)$ is defined as [1]

$$L_D(\omega) \equiv \frac{1}{\sqrt{\pi}\omega_D} \cdot \exp\left[-\frac{\Delta\omega^2}{\omega_D^2}\right]$$

where frequency detuning $\Delta\omega$, ω_D Doppler broadening parameter.

1.2.19 Definition

Lorentzian shape $L_L(\omega)$ is defined as [1]

$$L_L(\omega) \equiv \frac{w/\pi}{w^2 + (\Delta\omega - d)^2}$$

1.2.20 Theorem

Lets assume isolated line. Then Lorentzian shape may be used. [1]

Without proof.

1.2.21 Definition

Voigt shape $L_C(\omega)$ is defined as convolution of Gaussian (Doppler) shape and Lorentzian shape [1]

$$L_C(\omega) = \int_{-\infty}^{\infty} L_D(\Delta\omega')L(\Delta\omega - \Delta\omega')d\Delta\omega'$$

1.2.22 Definition

Source function S is defined for continuum system $\mathcal{S}_c$ with emission coefficient ε and absorption coefficient κ as [1]

$$S \equiv \frac{\varepsilon}{\kappa}$$

1.2.23 Theorem

Lets assume system with absorption coefficients κ_i for various processes i. Then total absorption coefficient κ meets

$$\kappa = \sum_i \kappa_i$$

Without proof.

1.2.24 Definition

Absorption coefficient κ is defined for continuum system $\mathcal{S}_c$ with cross-sections $\sigma_n(E_n)$ and particle densitites N_n as [1]

$$\kappa = \sum_n \sigma_n(E_n) \cdot N_n$$

1.2.25 Definition

Rate coefficient $\langle \sigma v \rangle [m^3 s^{-1}]$ is defined as

$$\langle \sigma v \rangle \rho_j \rho_s = r$$

where $r[m^{-3}s^{-1}]$ density of reactions, $\rho_j[m^{-3}]$ density of one particle type, $\rho_s[m^{-3}]$ density of second particle type.

1.3 Physical device

1.3.1 Definition

Physical device $\mathcal{P}$ is defined as ordered set of particle density $\rho(t, \vec{x})$ and evolution function $f : \mathcal{S}_c \to \mathcal{S}_c$

$$\mathcal{P} \equiv \{\rho(t, \vec{x}), f\}$$

1.3.2 Definition

Single quantity device is physical device, for which evolution function $f : \mathcal{S}_c \to \mathcal{S}_c$ becames scalar function

$$y = y(x(t))$$

1.3.3 Definition

Linear device is single quantity device, for which function $y = y(x(t))$ follows [2]

$$\sum_i \alpha_i y_i(t) = \sum_i \alpha_i x_i(t)$$

where $y_i = y_i(x_i(t))$.

1.3.4 Definition

Time invariant device is single quantity device, for which function $y = y(x(t))$ meets [2]

$$\forall t_0 \qquad y(t - t_0) = y(x(t - t_0))$$

where t is time.

1.3.5 Theorem

Lets assume linear time-invariant device with input, resp. output power signal $P_{SRC}(t)[W], \mathcal{S}_{AMP}(t)[W]$. Then exists so-called *response function* $h(t)$ such follows [2]

$$\mathcal{S}_{AMP}(t) = P_{SRC}(t) * h(t) \tag{1.1}$$

Without proof.

1.3.6 Theorem

Lets assume linear time-invariant device with input, resp. output power signal $P_{SRC}(t)[W], \mathcal{S}_{AMP}(t)[W]$. Then the relation from T.1.3.5 may be approximated for conditions f_j as

$$\mathcal{S}_{AMP}(t) = c_{DIA} \cdot P_{SRC}(t)$$

where $c_{DIA} \in \mathbb{R}$ is *total scalar diagnostics coefficient*.

Proof:

Directly from T.1.3.5 and convolution definition D.1.1.4.

1.3.7 Theorem

Lets assume diagnostics with $\rho_{DIA}(t, \vec{x})$ (probability density of its particles, but usually just a blueprint) with total scalar diagnostics coefficient c_{DIA}. Then for each diagnostics part $i \in \widehat{N}$ with

$$\rho_i(t, \vec{x}) \subset \rho_{DIA}(t, \vec{x}) \qquad \wedge \qquad \forall i, j : i \neq j : \qquad \rho_i \cap \rho_j = 0$$

exists *partial scalar diagnostics coefficient* $c_i \in \mathbb{R}$ such

$$c_{DIA} = \prod_{i=1}^{N} c_i \cdot c_\infty$$

where $c_\infty \in \mathbb{R}$ called *scalar diagnostics coefficients of unknown* corresponds to undescribed (= no theory to calculate a c_i) diagnostics parts $\rho_\infty(t, \vec{x})$. In ideal case $c_\infty \to 1$.

Proof:

From linearity and additivity.

1.4 Plasma

1.4.1 Definition

Plasma $\mathcal{P}$ is defined as continuum system $\mathcal{S}_c$ with i particle types with densities $\rho_i(t, \vec{x})$, energy densities $e(t, \vec{x})$ in single volume Ω, which is quasineutral and has collective behaviour.

1.4.2 Definition

Tokamak $\mathcal{T}$ is defined as toroidal magnetic vessel, which meets

- non-zero toroidal magnetic field B_T
- non-zero poloidal magnetic field B_P
- $B_T \gg B_P$
- plasma inside
- non-zero toroidal electric current $\vec{j}(t, \vec{x})$

1.4.3 Definition

Plasma edge is defined in tokamak $\mathcal{T}$ as plasma $\mathcal{P}$ between separatrix and first wall. Standard quantities may be introduced:

- electron, ion and impurity densities $\rho_e(t, \vec{x}), \rho_i(t, \vec{x}), \rho_m(t, \vec{x}) : \mathbb{R}^4 \to \mathbb{R}$
- electron, ion and impurity temperatures $T_e(t, \vec{x}), T_i(t, \vec{x}), T_m(t, \vec{x}) : \mathbb{R}^4 \to \mathbb{R}$
- electromagnetic field $\vec{E}(t, \vec{x}), \vec{B}(t, \vec{x}) : \mathbb{R}^4 \to \mathbb{R}^3$

1.4.4 Definition

Particle p is defined as ordered set of position $\vec{x} \in \mathbb{R}^3$, charge $q \in \mathbb{Z}$, mass $m \in \mathbb{R}^+$, momentum $\vec{p} \in \mathbb{R}^3$, energy

$$p \equiv \{\vec{x}, q, m, \vec{p}, E\}$$

1.4.5 Definition

Electromagnetic wave $\mathcal{W}$ alias photon is defined as ordered set of amplitude $A(t, \vec{x}) : \mathbb{R}^4 \to \mathbb{R}$ and phase $\varphi(t, \vec{x}) : \mathbb{R}^4 \to \mathbb{R}$

$$\mathcal{W} \equiv \{A(t, \vec{x}), \varphi(t, \vec{x})\}$$

1.4.6 Definition

Frequency ω of wave $\mathcal{W}$ is defined as

$$\omega \equiv \frac{\partial \varphi(t, \vec{x})}{\partial t}$$

1.4.7 Theorem

Lets assume a photon $\mathcal{W}$. Then its energy as particle meets

$$E \equiv \hbar\omega$$

1.4.8 Definition

Wave vector $\vec{k}$ of a photon $\mathcal{W}$ is defined as

$$\vec{k} \equiv \frac{\varphi(t, \vec{x})}{\vec{x}}$$

1.4.9 Definition

Wavelength λ of a photon $\mathcal{W}$ is defined as

$$\lambda \equiv \frac{2\pi}{|\vec{k}|}$$

1.4.10 Definition

Bremsstrahlung is process at Fig.1.4. Coulomb interaction between two charged particles results in their (de)acceleration and photon $\mathcal{W}$ is emmited.

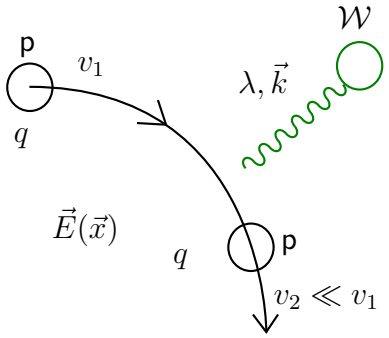

Figure 1.4: Bremsstrahlung schema

1.4.11 Theorem

Lets assume bremsstrahlung of electron on ion with collision parameter b and velocity v. Then emmited photon energy $E[J]$ meets [3]

$$E = \frac{Z^2 e^6}{48\pi^3 \varepsilon_0^3 c^3 m_e^2} \frac{1}{b^3 v}$$

1.4.12 Definition

Line radiation is process at Fig.1.4.12. Atom nucleus with excited electron layer $\mathcal{X}_1^*$ releases photon $\mathcal{W}$ with energy $E_\mathcal{W}$ and pass to excited $\mathcal{X}_2^*$ or ground state $\mathcal{X}_2$ with lower energy $E(X_1) > E(X_2)$.

$$E_\mathcal{W} = E(X_2) - E(X_1) \tag{1.2}$$

1.4.13 Definition

Effective ionic charge is defined for plasma with densitites $n_\alpha(t, \vec{x})$ and electric charges Z_α as

$$Z_{eff} \equiv \frac{\sum_j n_j Z_j^2}{\sum_j n_j Z_j}$$

1.4.14 Theorem

Lets assume plasma with temperature T and plasma atoms with ionization energy E_∞. Then bremsstrahlung becames dominant over recombination, when [1]

$$kT \gg E_\infty$$

Without proof.

1.4.15 Theorem

Lets assume steady-state radiation fields. Lets neglect refractive effects. Then for directional spectral intensity $I(\omega, \Omega)$ happens

$$dI(\omega, \Omega) = [\varepsilon(\omega, \Omega) - \kappa I(\omega, \Omega)]dx$$

where $\varepsilon(\omega, \Omega)$ emission coefficient, κ absorption coefficient, x is distance along the line of sight.

1.4.16 Definition

Plasma sheath is continuous plasma region $\Omega_{psh} \in \mathbb{E}^3$ wide several Debaye lengths $L = c \cdot \lambda_D$ along tokamak wall W with strong change of electric potential ϕ, see Fig.1.5.

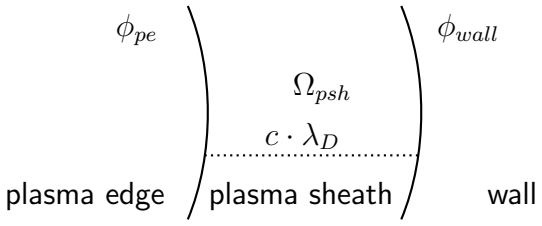

Figure 1.5: Plasma sheath schema

1.4.17 Theorem

Lets assume plasma sheath. Then charged plasma edge particles are accelerated towards the wall.

Proof:

Directly from definition due to electric potential change.

1.4.18 Theorem

Lets assume plasma edge near wall, see Fig.1.6. Then exists particle flux $\Phi_1(t, \vec{x})$ from plasma edge to wall. Wall absorbs their energy and neutralizes them. Particle flux $\Phi_2(t, \vec{x})$ is backscattered. Particle flux $\Phi_3(t, \vec{x})$ is trapped in the wall. Exists probability P of releasing trapped particle back as particle flux Φ_4.

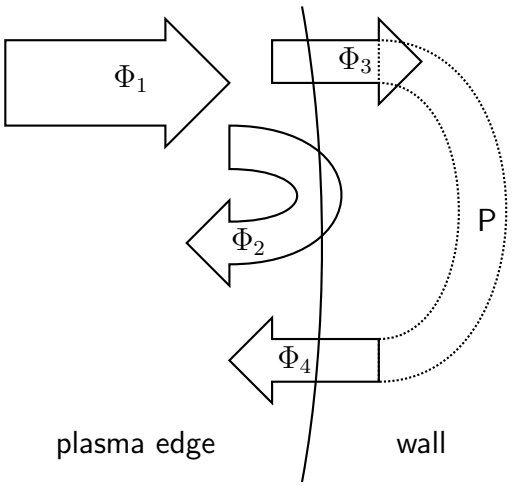

Figure 1.6: Recycling schema.

1.4.19 Theorem

Lets assume a momentum gain for atom in wall. Then it may be released into plasma edge.

Without proof.

1.4.20 Theorem

Lets assume electric discharge between plasma edge and wall due to plasma sheath potential drop. Then wall atom may be released into plasma edge.

Without proof.

1.4.21 Theorem

Lets assume plasma with final-state perturbations neglected and pure Coulomb scattering only. Then [1] for line width w

$$w = \langle \frac{1}{2} N_e v \sigma \rangle$$

where N_e electron density, v electron velocity and σ cross-section.

Chapter 2

VIS Multichannel diagnostics

2.1 CCD detector

2.1.1 Definition

CCD detector is single linear time-invariant physical device with evolution function

$$\mathcal{S}_{CCD} = c_{CCD} \cdot \int_{\mathbb{R}^+} ps(\lambda) \cdot P_{CCD}(t, \lambda) d\lambda$$

where $\mathcal{S}_{CCD}[W]$ is power of generated electric signal, $P_{CCD}(t, \lambda)[Wm^{-1}]$ is spectral power of incoming photon beam on the CCD detector, $ps(\lambda)[A/W]$ is *photosensitivity* function, $c_{CCD}[V]$ *sensitivity constant* and $t[s]$ is time.

2.1.2 Theorem

Lets assume CCD detector array composed of e elements processing powers from optical cable composed of e optical fibres, see Fig.2.1. Then kth CCD element incident power $P^{(k)}_{CCD}(t)$ is composed of power from kth optical fibre and partially overlapping powers from neigthbour k+1th and k-1th optical fibres, e.g. $P^{(k)}_{OFE}(t), P^{(k-1)}_{OFE}(t), P^{(k+1)}_{OFE}(t)$, where OFE stands for Optical Fibre End.

$$\forall k \in \hat{e} \qquad P^{(k)}_{CCD} = \alpha_k \cdot P^{(k-1)}_{OFE}(t) + \beta_k \cdot P^{(k)}_{OFE} + \gamma_k \cdot P^{(k+1)}_{OFE}(t)$$

where $\alpha_k, \beta_k, \gamma_k$ are *coefficients of overlapping*.

Without proof.

2.2 Amplifier

2.2.1 Definition

Power amplifier is single linear time-invariant physical device, which amplifies electric current power

$$\mathcal{S}_{AMP} = \mathcal{S}_{AMP}(t, \mathcal{A}_{AMP}, \mathcal{S}(t)) \qquad \forall t : \mathcal{S}_{AMP}(t) \gg \mathcal{S}(t)$$

where $\mathcal{S}(t)[W]$ is input power of electric signal, $\mathcal{S}_{AMP}(t)[W]$ amplified output power of electric signal, $\mathcal{A}_{AMP}[-] \in \mathbb{R}$ is *amplification* and $t[s]$ time.

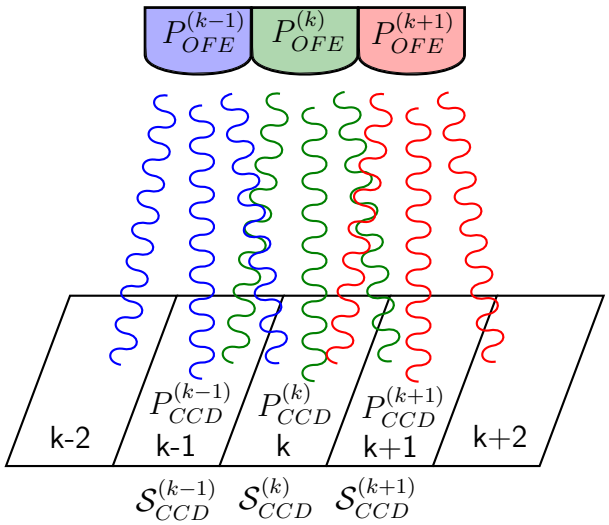

Figure 2.1: Overlapping between optical fibers and CCD array

2.2.2 Theorem

Lets assume power amplifier with impulse response function $h(t) = \Theta(t) \cdot \mathcal{A}_{AMP} \cdot e^{-t/\tau}$ where $\mathcal{A}_{AMP}[-]$ amplification and $\tau \in \mathbb{R}$ *response constant*. Then its signal output power $\mathcal{S}_{AMP}(t)$ of square signal input power $\mathcal{S}(t)$ with amplitude $\bar{\mathcal{S}}$, start and end times t_0, t_1 meets

$$\mathcal{S}_{AMP}(t) = \bar{\mathcal{S}} \cdot \mathcal{A}_{AMP} \cdot \tau \cdot \Theta(\min\{t_0, t-t_0\}) \cdot \left[1 - e^{-\frac{t-t_0}{\tau}}\right] - A \cdot \tau \cdot \Theta(\min\{t, t-t_1\}) \cdot \left[1 - e^{-\frac{t-t_1}{\tau}}\right]$$

Proof:

For linear time invariant amplifier

$$\mathcal{S}_{AMP}(t) \overset{T.1.3.5}{=} \mathcal{S}(t) * h(t) \qquad \Big/ \mathcal{S}(t) = \mathcal{S}_{sq}(t), \qquad \Big/ h(t) = \Theta(t) \cdot \mathcal{A}_{AMP} \cdot e^{-\frac{t}{\tau}}$$

$$\mathcal{S}_{AMP}(t) = \mathcal{S}_{sq}(t) * \Theta(t) \cdot \mathcal{A}_{AMP} \cdot e^{-\frac{t}{\tau}} \qquad \Big/ \mathcal{S}_{sq}(t) \overset{D.1.1.5}{=} \bar{\mathcal{S}} \cdot [\Theta(t-t_0) - \Theta(t-t_1)]$$

$$\mathcal{S}_{AMP}(t) = \bar{\mathcal{S}} \cdot [\Theta(t-t_0) - \Theta(t-t_1)] * \Theta(t) \cdot \mathcal{A}_{AMP} \cdot e^{-\frac{t}{\tau}} \qquad \Big/ (f*g)(x) \overset{D.1.1.4}{=} \int_{\mathbb{R}} f(s) \cdot g(x-s) ds$$

$$\begin{aligned}
\mathcal{S}_{AMP}(t) &= \int_{\mathbb{R}} \bar{\mathcal{S}} \cdot [\Theta(s-t_0) - \Theta(s-t_1)] \cdot \Theta(t-s) \cdot \mathcal{A}_{AMP} \cdot e^{-\frac{t-s}{\tau}} ds = \\
&= \Big| \Theta(t-s) \Rightarrow s \in (-\infty, t) \wedge t > 0 \Rightarrow \Theta(t) \Big| = \\
&= \bar{\mathcal{S}} \cdot \mathcal{A}_{AMP} \cdot \Theta(t) \left[\int_{-\infty}^{t} \Theta(s-t_0) e^{-\frac{t-s}{\tau}} ds - \int_{-\infty}^{t} \Theta(s-t_1) e^{-\frac{t-s}{\tau}} ds \right] = \\
&= \Big| \Theta(s-t_i) \Rightarrow s \in (t_i, t) \wedge t_i < t \Rightarrow \Theta(t-t_i) \Big| = \\
&= \bar{\mathcal{S}} \cdot \mathcal{A}_{AMP} \Theta(t) \left[\Theta(t-t_0) \int_{t_0}^{t} e^{-\frac{t-s}{\tau}} ds - \Theta(t-t_1) \int_{t_1}^{t} e^{-\frac{t-s}{\tau}} ds \right] = \\
&= \Big| z = -\frac{t-s}{\tau} \Rightarrow dz = \frac{ds}{\tau}, \Theta(t) \cdot \Theta(t-t_i) \overset{T.1.1.3}{=} \Theta(\min\{t, t-t_i\}) \Big| =
\end{aligned}$$

$$= \bar{\mathcal{S}} \cdot \mathcal{A}_{AMP}\Theta(t)\Theta(t-t_0)\int_{-\frac{t-t_0}{\tau}}^{0} e^z \tau dz - \bar{\mathcal{S}} \cdot \mathcal{A}_{AMP}\Theta(t)\Theta(t-t_1)\int_{-\frac{t-t_1}{\tau}}^{0} e^z \tau dz =$$

$$= \bar{\mathcal{S}} \cdot \mathcal{A}_{AMP}\Theta(\min\{t, t-t_0\})\tau[e^z]_{-\frac{t-t_0}{\tau}}^{0} - \bar{\mathcal{S}} \cdot \mathcal{A}_{AMP}\Theta(\min\{t, t-t_1\})\tau[e^z]_{-\frac{t-t_1}{\tau}}^{0}$$

$$\mathcal{S}_{AMP}(t) = \bar{\mathcal{S}} \cdot \mathcal{A}_{AMP} \cdot \tau \cdot \Theta(\min\{t_0, t-t_0\}) \cdot \left[1 - e^{-\frac{t-t_0}{\tau}}\right] -$$

$$\bar{\mathcal{S}} \cdot \mathcal{A}_{AMP} \cdot \tau \cdot \Theta(\min\{t, t-t_1\}) \cdot \left[1 - e^{-\frac{t-t_1}{\tau}}\right] \qquad Q.E.D.$$

2.3 Optical fibres

2.3.1 Theorem

Lets assume photon beam with input power $P_{OFS}(t)[W]$ coming throught a homogenous optical fibre with length $l[m]$ and output power $P_{OFE}(t)$ (OFS optical fiber start, OFE optical fiber end). Then exists length damping $a[dB/km]$ constant, which meets

$$P_{OFE}(t) = 10^{-a \cdot l} P_{OFS}(t)$$

Proof:

Optical fibre is linear and invariant device, thus from its definition

$$\sum_i \alpha_i P_o(t) = \sum_i \alpha_i P_o(t)$$

which for single photon beam gives

$$P_{OFE}(t) = \alpha \cdot P_{OFS}(t) \qquad \Big/ : P_{OFS}(t)$$

$$\frac{P_{OFE}(t)}{P_{OFS}(t)} = \alpha \qquad \Big/ \log_{10}$$

$$\log_{10}\left(\frac{P_{OFE}(t)}{P_{OFS}(t)}\right) = \log_{10}\alpha \qquad \Big/ A \equiv -\log_{10}\alpha = const., A > 0$$

$$\log_{10}\left(\frac{P_{OFE}(t)}{P_{OFS}(t)}\right) = -A \qquad \Big/ A = \int a(l)dl$$

For homogenous optical fibre $\partial a/\partial l = 0$, thus

$$\log_{10}\left(\frac{P_{OFE}(t)}{P_{OFS}(t)}\right) = -\int a dl \qquad \Big/ \int a dl = a\int dl = a \cdot l$$

$$\log_{10}\left(\frac{P_{OFE}(t)}{P_{OFS}(t)}\right) = -a \cdot l \qquad \Big/ 10^{-}$$

$$\frac{P_{OFE}(t)}{P_{OFS}(t)} = 10^{-a \cdot l} \qquad \Big/ \cdot P_{OFS}(t)$$

$$P_{OFE}(t) = 10^{-a \cdot l} \cdot P_{OFS}(t) \qquad Q.E.D.$$

2.4 Observation area

2.4.1 Theorem

Lets assume boundary between optical fiber and vacuum, see Fig.2.2. Lets assume incoming spectral wave-vector-dependent power $P_{INC}(t, \lambda, \vec{k})$ in vacuum and spectral power $P_{OFS}(t, \lambda)$ inside at the Optical Fiber Start. Then exists

$$\Omega \subset \mathbb{R}^3 : \qquad P_{OFS}(t, \lambda) = \int_{\Omega} P_{INC}(t, \lambda, \vec{k}) d\vec{k}$$

called *set of allowed wave vectors*.

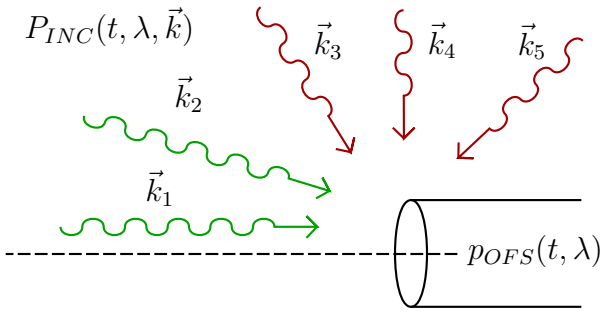

Figure 2.2: Fiber-vacuum boundary: green waves are allowed into the fiber, red are not

Without proof.

2.4.2 Theorem

Lets assume optical fiber at position $\vec{x}_{OF}$ with its axis $\vec{a}$ with outcoming photon beam, solid plane at position $\vec{S}_{plane}$ under angle α, β to the fiber axis and illuminated area $\vec{S}_{ill}$ at the solid plane, see Fig.2.3. Lets neglect difference between incoming and outgoing photon wave from the optical fiber. Then the set of allowed wave vectors meets

$$\Omega = \{\vec{k} \in \mathbb{R}^3 : \qquad \exists \vec{x}_{ill} \in \vec{S}_{ill} \qquad \vec{k} = \vec{x}_{ill} - \vec{x}_{of}\}$$

Without proof.

2.4.3 Theorem

Lets assume isotropic static light point SouRCe in $\vec{x}_{SRC}$ with spectral wave-vector-dependent power $P_{SRC}(t, \lambda, \vec{k})$ in the space with incoming spectral wave-vector dependent power $P_{INC}(t, \lambda, \vec{k})$, see Fig.2.4. Then exists

$$\Omega_{SRC} \subset \mathbb{R}^3 \qquad P_{INC}(t, \lambda, \vec{k}) = \int_{\Omega_{SRC}} P_{SRC}(t, \vec{x}, \vec{k}) d\vec{k}$$

called *set of created vectors*.

Without proof.

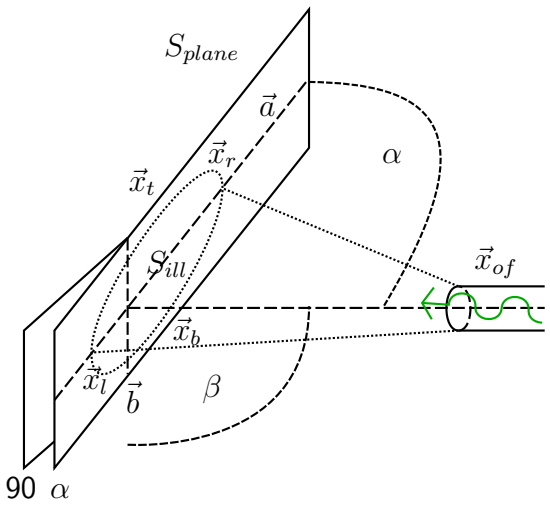

Figure 2.3: Allowed vectors

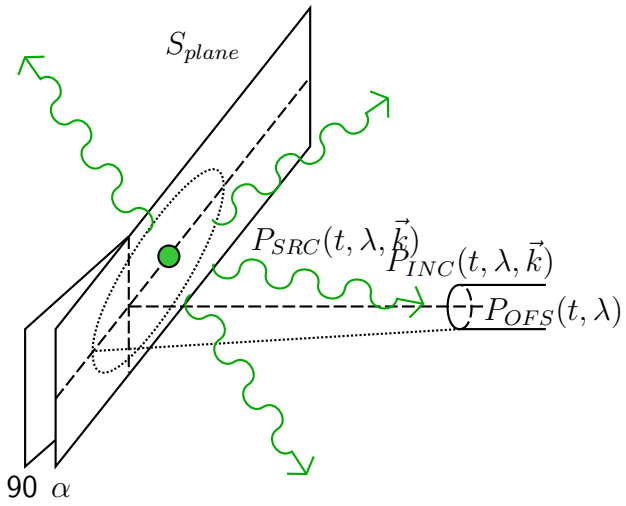

Figure 2.4: Created vectors

2.5 Calibrations

2.5.1 Definition

VIS Multichannel diagnostics is defined as physical device with $\rho_{VIS}(t, \vec{x})$ defined in articles [5] [7].

2.5.2 Theorem

Lets assume VIS Multichannel diagnostics on tokamak COMPASS in year 2013. Then according to T.1.3.7 for its evolution function $\mathcal{S}_{AMP} = \mathcal{S}_{AMP}(t, P_{SRC}(t, \lambda, \vec{k}))$ exist simple approximation by scalar coefficients

- $P_{INC}(t, \lambda) = c_{OBS} \cdot P_{SRC}(t, \lambda, \vec{k})$
- $P_{OFS}(t, \lambda) = c_{OBS2} \cdot P_{INC}(t, \lambda)$
- $P_{OFE}(t, \lambda) = c_{OF} \cdot P_{OFS}(t, \lambda)$

- $P_{CCD}(t,\lambda) = c_{ALG} \cdot P_{OFE}(t,\lambda)$
- $\mathcal{S}_{CCD}(t) = c_{CCD} \cdot P_{CCD}(t,\lambda)$
- $\mathcal{S}_{AMP}(t) = c_{AMP} \cdot \mathcal{S}_{CCD}(t)$

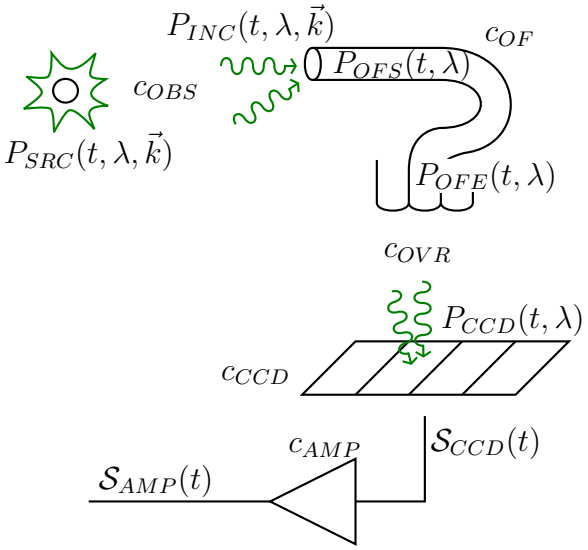

Figure 2.5: VIS Diagnostics Decomposition

Proof:

Directly from VIS Multichannel's $\rho_{VIS}(t,\vec{x})$, where optical fibers with its $\rho_{OF}(t,\vec{x})$, CCD detector with $\rho_{CCD}(t,\vec{x})$ and amplifier with $\rho_{AMP}(t,\vec{x})$ may be found, see VIS schema in Fig.2.5. The approximation is described in T.1.3.7.

2.5.3 Theorem - VIS CCD photosensitivity

Lets assume the VIS Multichannel CCD detector on tokamak COMPASS in 2013 year with its function

$$\mathcal{S}_{CCD}(t) = c_{CCD} \cdot \int_{\mathbb{R}^+} ps(\lambda) \cdot P_{CCD}(t,\lambda) d\lambda$$

Then its photosensitivity function $ps(\lambda)$ is at Fig.2.6.

Provided by manufacturer.

2.5.4 Theorem - CCD relative sensitivity calibration

Lets assume both VIS Multichannel CCD detector arrays each composed of 35 CCD elements on tokamak COMPASS in 2013 year with its function

$$\mathcal{S}^{ae}_{CCD}(t) = c^{ae}_{CCD} \cdot \int_{\mathbb{R}^+} ps(\lambda) \cdot P^{ae}_{CCD}(t,\lambda) d\lambda \qquad a \in \widehat{2}, e \in \widehat{35}$$

Then the relative calibration constants $c^{ae}_{CCD}/c^{a1}_{CCD}$ are shown at Fig.2.7 and Fig.2.8.

Proof:

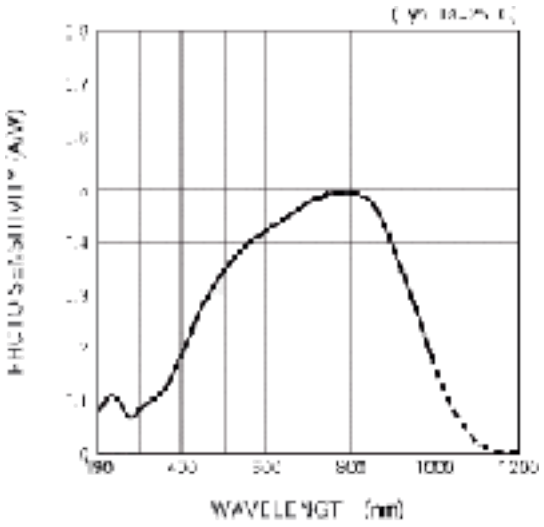

Figure 2.6: VIS CCD photosensitivity function $ps(\lambda[nm])[W/A]$

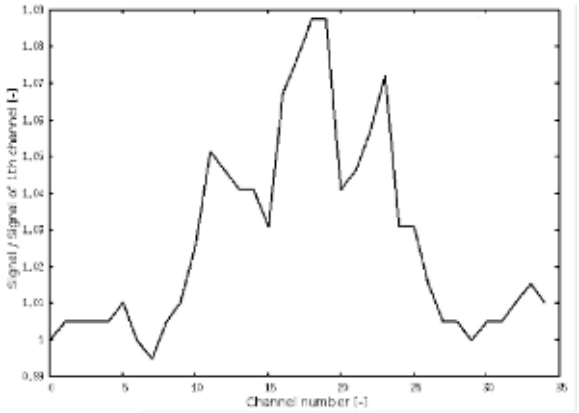

Figure 2.7: VIS1 CCD relative coefficients of calibration $c^{1e}_{CCD}/c^{11}_{CCD}$ [4]

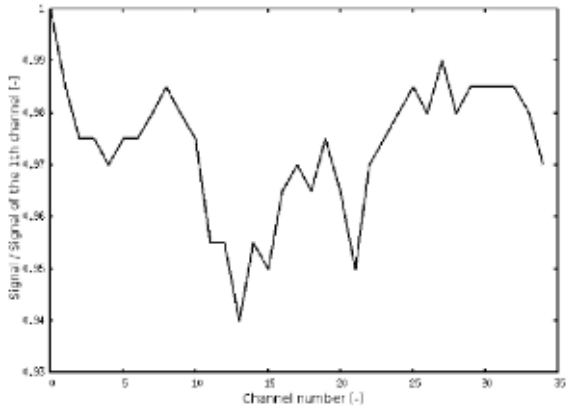

Figure 2.8: VIS2 CCD relative coefficients of calibration $c^{2e}_{CCD}/c^{21}_{CCD}$ [4]

Proved in [4].

2.5.5 Theorem - VIS CCD overlapping calibration

Lets assume both VIS CCD detector arrays with VIS optical cables on tokamak COMPASS in 2013 year. Then the relative coefficients of overlapping from T.2.1.2

$$a \in \widehat{2} \qquad \forall i \in \widehat{35} \qquad \frac{\alpha_i^a}{\alpha_{rc}^a}, \frac{\beta_i^a}{\beta_{rc}^a}, \frac{\gamma_i^a}{\gamma_{rc}^a}$$

where $rc = 4$ for first array $a = 1$ and $rc = 1$ for second array $a = 2$ are shown in Fig.2.9, Fig.2.10 [4].

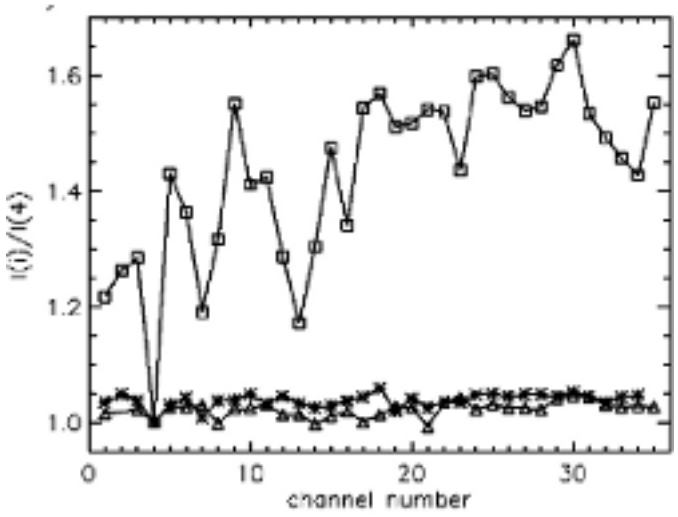

Figure 2.9: VIS1 relative coefficients of overlapping, [4]

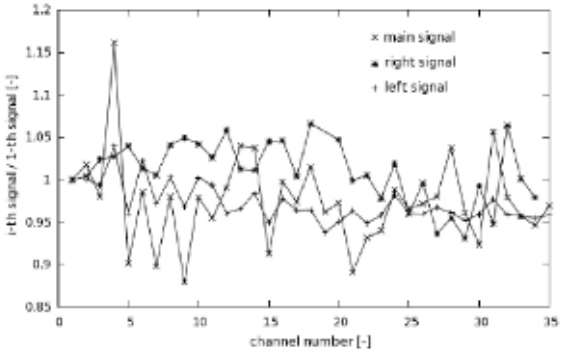

Figure 2.10: VIS2 relative coefficients of overlapping, [4]

Proof:

Calibration details may be found in [4].

2.5.6 Theorem - Amplifier calibration for response constant

Lets assume the VIS Amplifier on tokamak COMPASS in 2013 year. Then the amplifier output signal is according to T.2.2.2

$$\mathcal{S}_{AMP}(t) = \bar{\mathcal{S}} \cdot \mathcal{A}_{AMP} \cdot \tau \cdot \Theta(\min\{t_0, t - t_0\}) \cdot \left[1 - e^{-\frac{t-t_0}{\tau}}\right] - A \cdot \tau \cdot \Theta(\min\{t, t - t_1\}) \cdot \left[1 - e^{-\frac{t-t_1}{\tau}}\right]$$

and its response constant is

$$\tau = 4.9225 \cdot 10^{-7} s$$

Proof:

By calibration in [4].

2.5.7 Theorem

Lets assume VIS Multichannel diagnostics. Then for last Nth diagnostics part related to observation geometry Fig.2.11 the relative coefficients c_N^{aj}/c_N^{aref} are plotted in Fig.2.12,2.13.

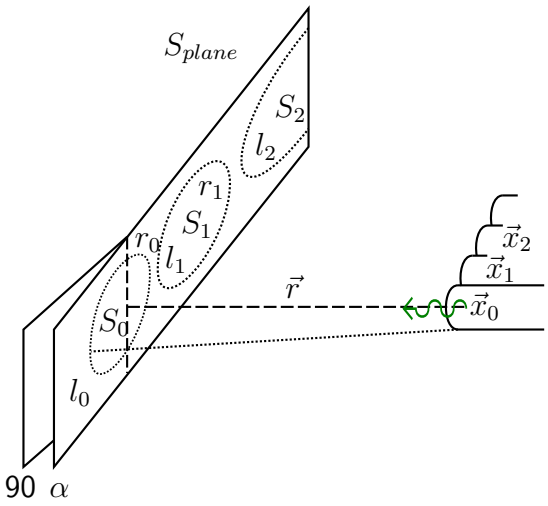

Figure 2.11: VIS Mutlichannel diagnostics observation geometry

Proof:

The proof is several theoretical steps and measured geometry values:

1. Light path x between light source and fiber may be calculated from light source position x_i, projection plane angle α and reference channel axial distance x_0 as

$$x = \sqrt{x_i^2 + x_0^2 - 2|x_i|x_0 \cos\left(\frac{\pi}{2} + \alpha \mathrm{sgn} x_i\right)}$$

which may be derived from Fig.2.14. For $x_i > 0$ thus

$$\begin{aligned} \eta &= \pi - \epsilon \qquad \Big/ \pi = \alpha + \frac{\pi}{2} + \epsilon \\ \eta &= \pi - \left(\pi - \alpha - \frac{\pi}{2}\right) \\ \eta &= \frac{\pi}{2} + \alpha \end{aligned}$$

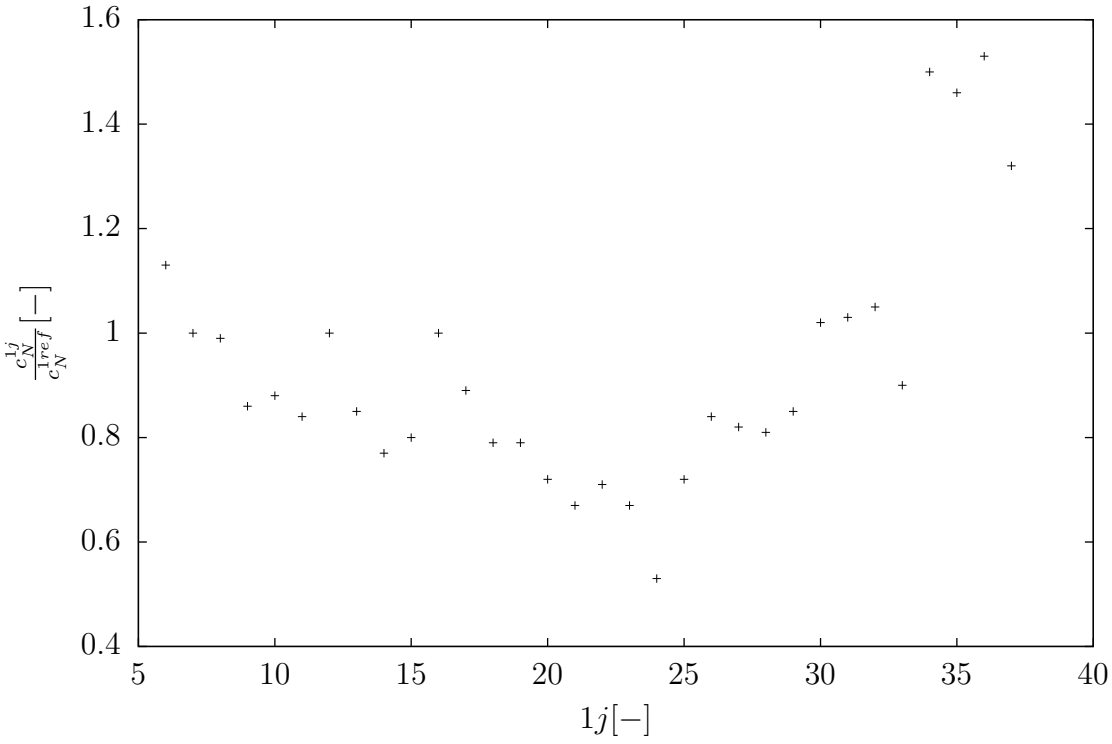

Figure 2.12: VIS BOT relative *scalar diagnostics coefficients* of observation issue from T.1.3.7

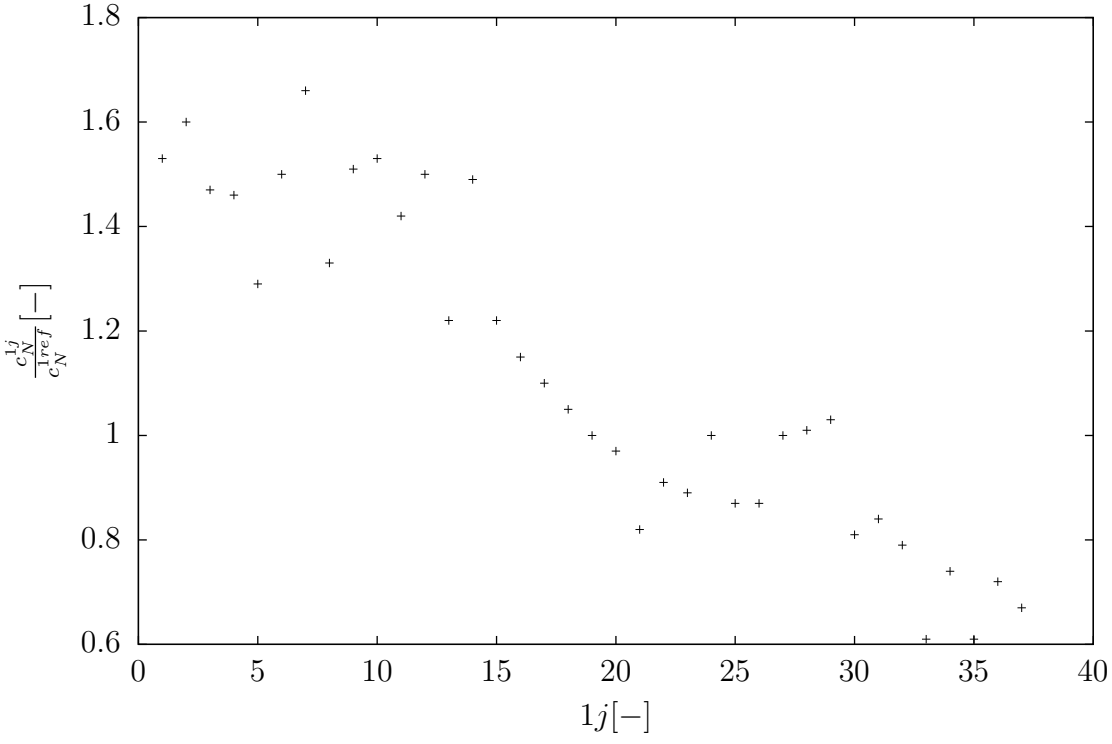

Figure 2.13: VIS TOP relative *scalar diagnostics coefficients* of observation issue from T.1.3.7

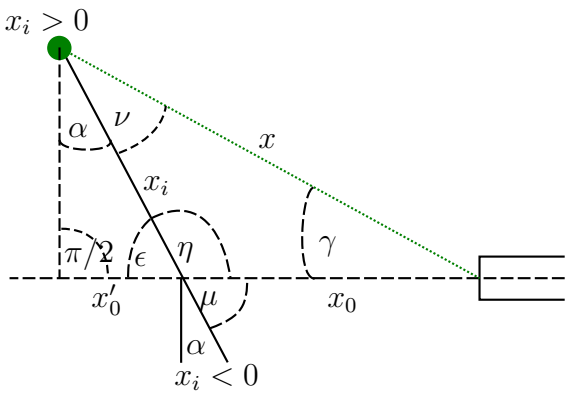

Figure 2.14: Light path calculation

and for $x_i < 0$

$$\mu = \frac{\pi}{2} - \alpha$$

Thus both expressions may be generalised as

$$\eta' = \begin{cases} \eta & x_i > 0 \\ \mu & x_i < 0 \end{cases}$$
$$\eta' = \frac{\pi}{2} + \alpha \mathsf{sgn} x_i$$

Thus, according to cosine theorem

$$x^2 = x_i^2 + x_0^2 - 2|x_i x_0| \cos \eta' \qquad \Big/ \eta' = \frac{\pi}{2} + \alpha \mathsf{sgn} x_i, \qquad \Big/ x_0 > 0$$
$$x^2 = x_i^2 + x_0^2 - 2|x_i| x_0 \cos\left(\frac{\pi}{2} + \alpha \mathsf{sgn} x_i\right) \qquad \Big/ \sqrt{}$$
$$x = \sqrt{x_i^2 + x_0^2 - 2|x_i| x_0 \cos\left(\frac{\pi}{2} + \alpha \mathsf{sgn} x_i\right)} \qquad Q.E.D.^1$$

2. Illuminated area S_i may be gained according to geometry from Fig.2.15 as sum of three parts: left half-circle, rectangle in middle and right half-circle

$$S_i = S_{left} + S_{middle} + S_{right} \qquad \Big/ S_{left} = \frac{1}{2}\pi h^2, S_{middle} = 2 \cdot h(r_i - l_i), S_{right} = \frac{1}{2}\pi h^2$$
$$S_i = \pi h^2 + 2h(r_i - l_i - 2h) \qquad Q.E.D.^2$$

3. Angle γ may be gained according to Fig.2.14 as

$$\gamma = \mathsf{arccos} \frac{x_0 + x_i \sin \alpha}{x}$$

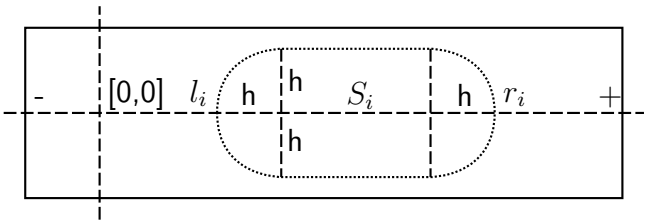

Figure 2.15: Illuminated area calcuation

which may be derived as

$$\cos\gamma = \frac{x_0 + x_0'}{x} \qquad \Big/ \sin\alpha = \frac{x_0'}{x_i}$$
$$\cos\gamma = \frac{x_0 + x_i \sin\alpha}{x} \qquad \Big/ \arccos$$
$$\gamma = \arccos\frac{x_0 + x_i \sin\alpha}{x} \qquad Q.E.D.^3$$

4. Angle θ may be gained according to Fig.2.16 and Fig.2.14 as

$$\theta = \gamma + \alpha$$

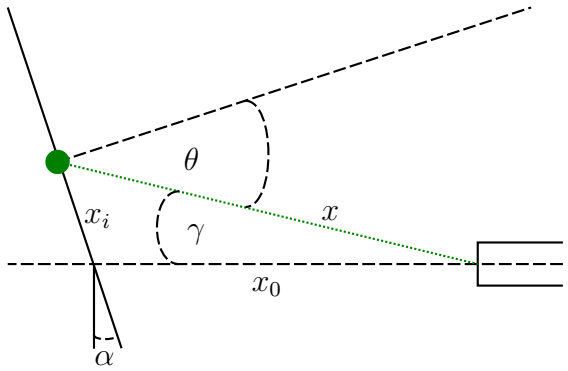

Figure 2.16: Top view

The relation may be prooved in the following way:

$$\pi = \gamma + \frac{\pi}{2} + \alpha + \nu \qquad \Big/ -\gamma - \frac{\pi}{2} - \alpha$$
$$\nu = \frac{\pi}{2} - \gamma - \alpha$$

$$\theta + \nu = \frac{\pi}{2} \qquad \Big/ -\nu$$
$$\theta = \frac{\pi}{2} - \nu \qquad \Big/ \nu = \frac{\pi}{2} - \gamma - \alpha$$
$$\theta = \frac{\pi}{2} - \frac{\pi}{2} + \gamma + \alpha$$
$$\theta = \gamma + \alpha \qquad Q.E.D.^4$$

5. Relative coefficients c_N^{aj}/c_N^{aref} of the observation geometry (see Figs.2.4,2.16) for a array, j element may be calculated as

$$\frac{c_N^{aj}}{c_N^{aref}} = \frac{S_{aj} \cdot \cos\theta_{aj} \cos\gamma_{aj} x_{a0}^2}{S_{aref} \cos\theta_{aref} \cos\gamma_{aref} x_{aj}^2}$$

Lets assume source power P_{SRC}^j coming out from jth optical fiber and incoming to the plane with power P_{PLN}^j. Then exists coefficient c_N^j

$$\begin{aligned}
P_{SRC}^{aj} \cdot c_N^{aj} &= P_{PLN}^{aj} \qquad \Big/ : P_{PLN}^{aref} = P_{SRC}^{aref} \cdot c_N^{aref} \\
\frac{P_{SRC}^{aj}}{P_{SRC}^{aref}} \cdot \frac{c_N^{aj}}{c_N^{aref}} &= \frac{P_{PLN}^{aj}}{P_{PLN}^{aref}} \qquad \Big/ \forall j,k \in \widehat{37} : P_{SRC}^j = P_{SRC}^k \\
\frac{c_N^{aj}}{c_N^{aref}} &= \frac{P_{PLN}^{aj}}{P_{PLN}^{aref}} \qquad \Big/ P \overset{T.1.2.5}{=} \iint L \cos\theta \cos\gamma x^{-2} dS_d dS_p \\
\frac{c_N^{aj}}{c_N^{aref}} &= \frac{\iint L \cos\theta^{aj} \cos\gamma^{aj} x_{aj}^{-2} dS_d dS_p}{\iint L \cos\theta^{aref} \cos\gamma^{aref} x_{aref}^{-2} dS_d dS_p} \qquad \Big/ L = \text{const.}, S_p = \text{const.} \\
\frac{c_N^{aj}}{c_N^{aref}} &= \frac{S_{aj} \cdot \cos\theta_{aj} \cos\gamma_{aj} x_{a0}^2}{S_{aref} \cos\theta_{aref} \cos\gamma_{aref} x_{aj}^2}
\end{aligned}$$

6. Measured geometry quantities are shown in Figs.2.17.2.18.2.19.2.20.2.21.2.22. Reference channels are for VIS BOT channel No.16 with $x_0^{1ref} = 149mm$, $\alpha^1 = 0.785rad$ and for VIS TOP channel No.19 with $x_0^{2ref} = 209mm$, $\alpha^2 = 0.349$. If used, the results in Figs.2.12.2.13 are prooved. Q.E.D.

2.5.8 Theorem

Lets assume VIS mutlichannel diagnostics. Then the relative *scalar diagnostics coefficients of unknown* $c_\infty^{aj}/c_\infty^{aref}$ for both arrays $a \in \widehat{2}$ and all 37 channels $j \in \widehat{37}$ are plotted in Fig.2.23,2.24.

Proof:

Directly from the T.1.3.7 and with respect to T.2.5.7, which calculates observation relative scalar diagnostics coefficients c_N^{aj}/c_N^{aref} (observation geometry problem is marked as the Nth diagnostics

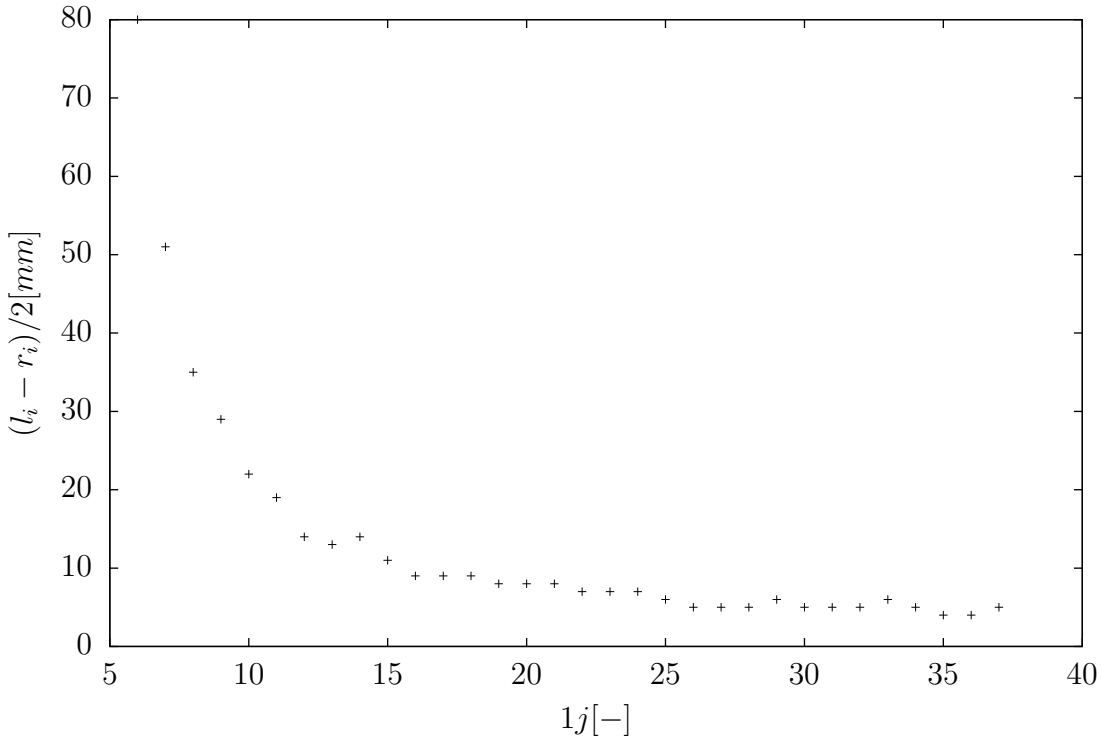

Figure 2.17: VIS BOT measured halfwidth $(l_i - r_i)/2$ according to Fig.2.11

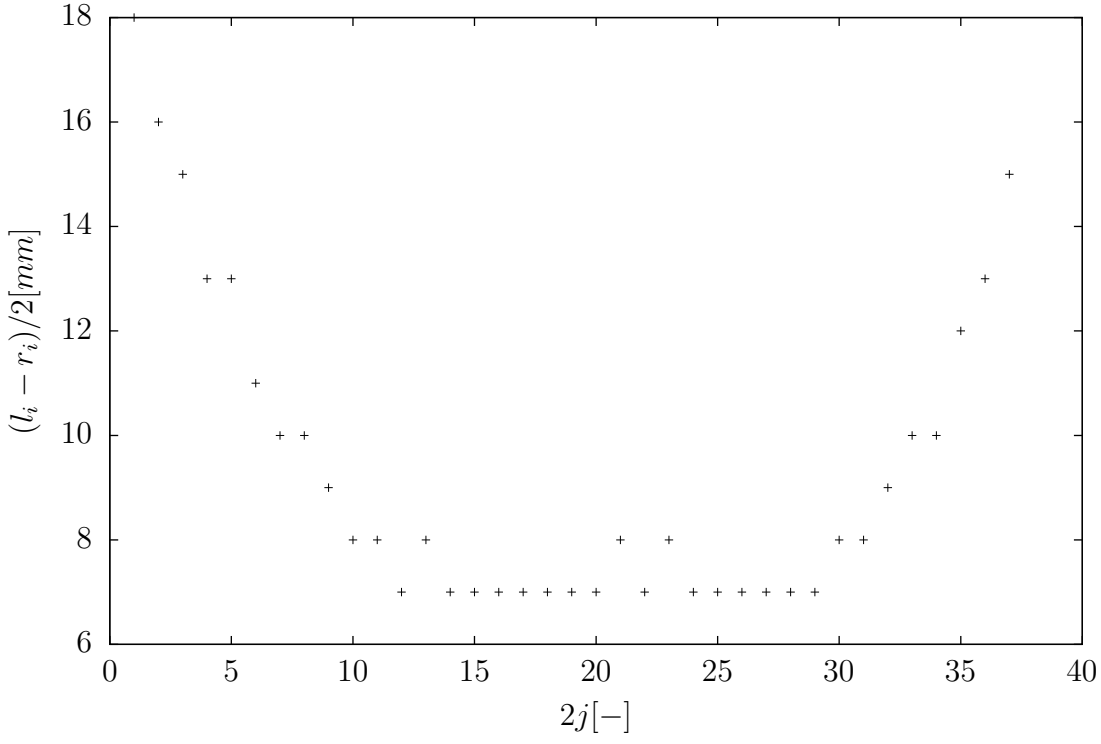

Figure 2.18: VIS TOP measured halfwidth $(l_i - r_i)/2$ according to Fig.2.11

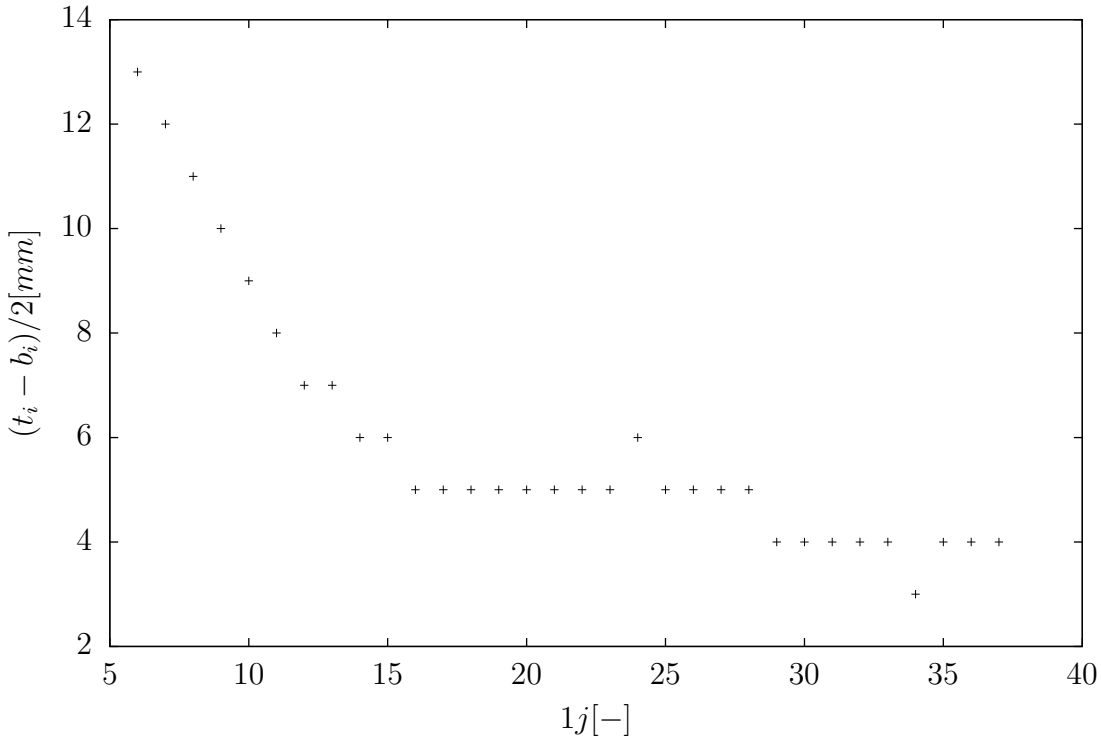

Figure 2.19: VIS BOT measured halfheight $(t_i - b_i)/2$ according to Fig.2.11

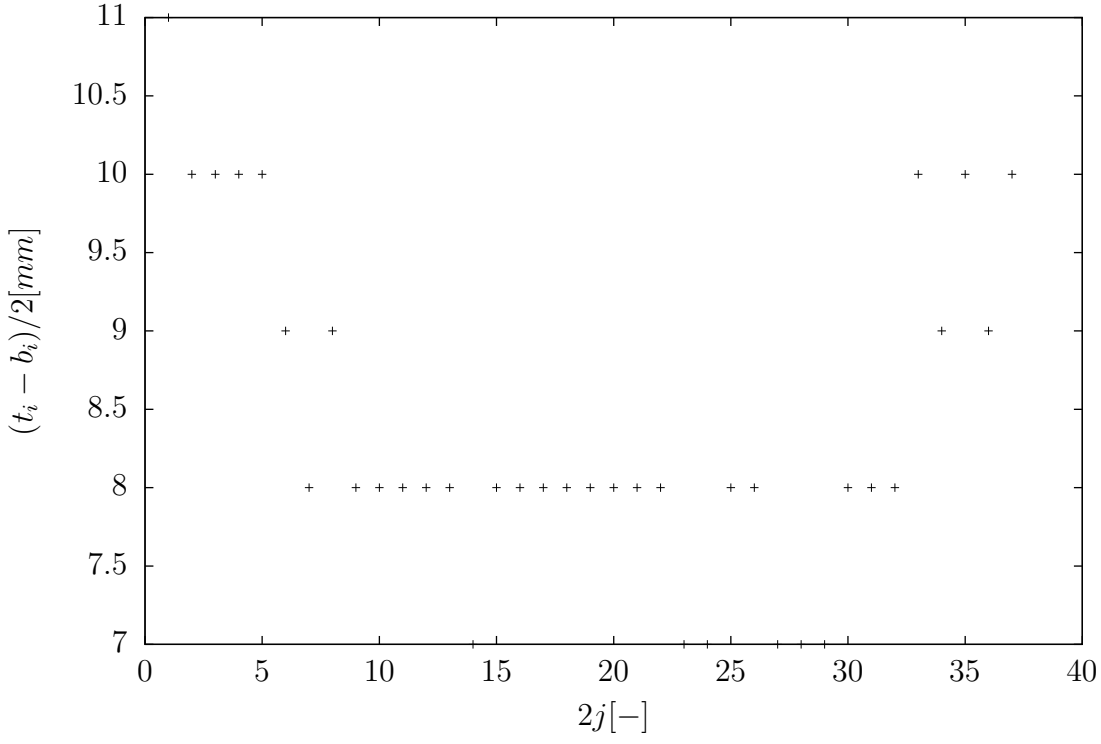

Figure 2.20: VIS TOP measured halfheight $(t_i - b_i)/2$ according to Fig.2.11

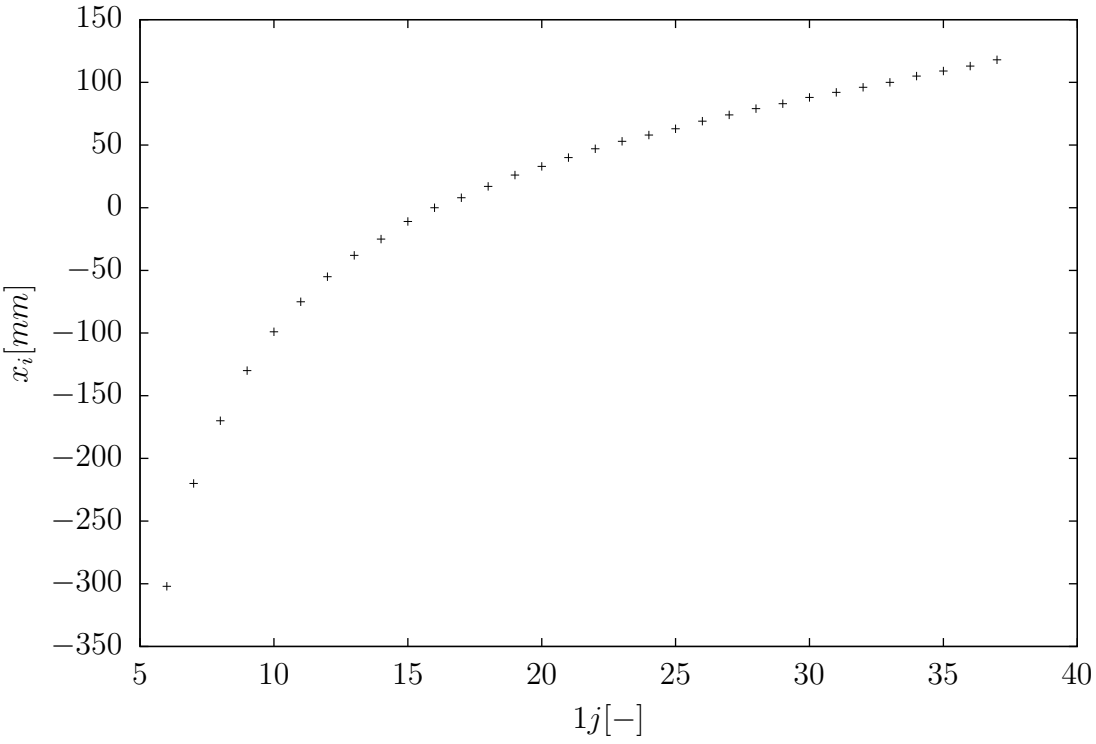

Figure 2.21: VIS BOT measured illuminated area center positions x_i

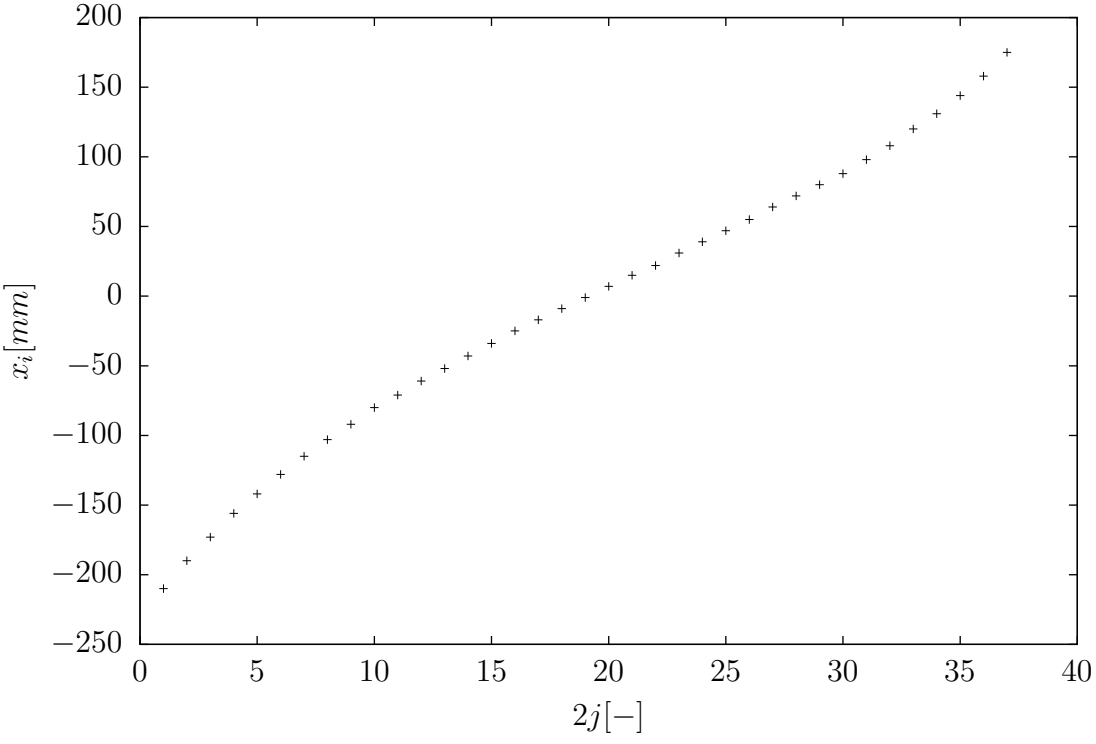

Figure 2.22: VIS TOP measured illuminated area center positions x_i

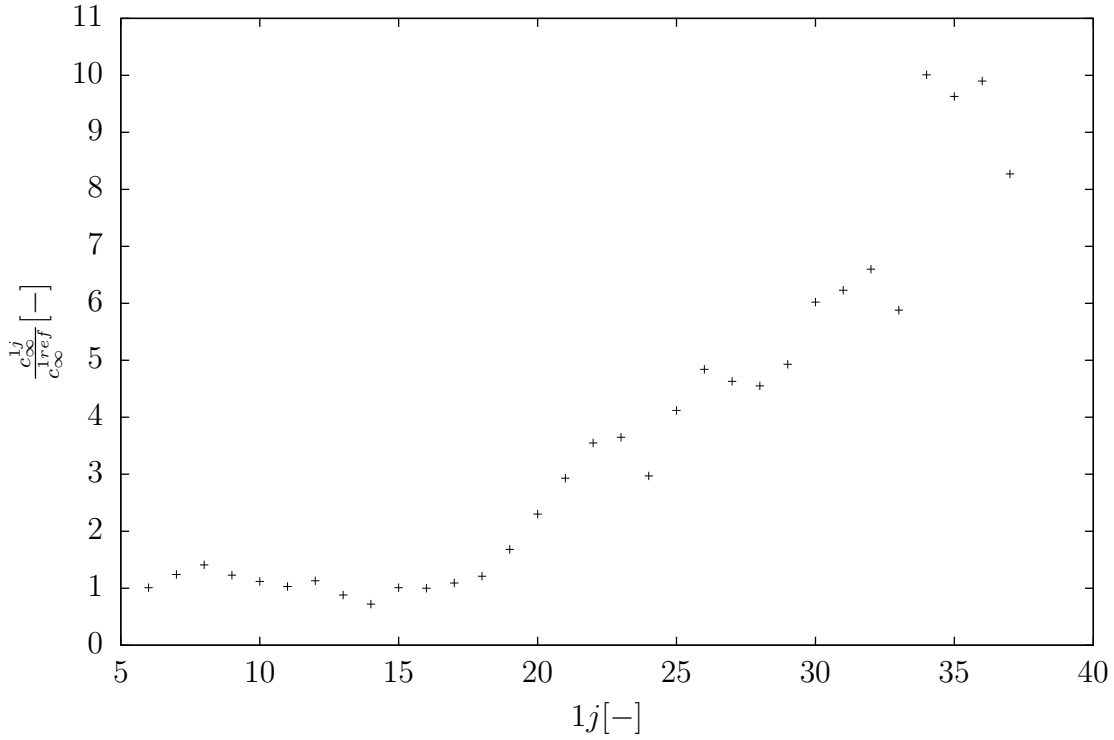

Figure 2.23: VIS BOT relative *scalar diagnostics coefficients of unknown* from T.1.3.7 to reference channel No.16

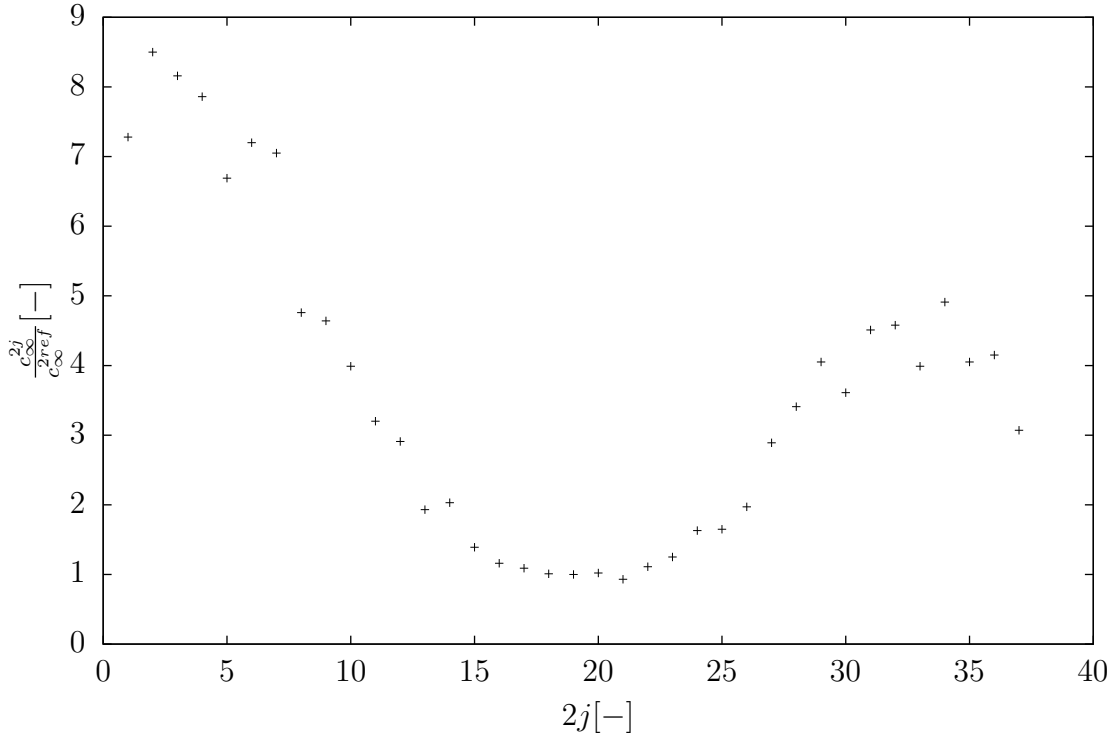

Figure 2.24: VIS TOP relative *scalar diagnostics coefficients of unknown* from T.1.3.7 to reference channel No.19

problem). Thus from T.1.3.6

$$\mathcal{S}(t) \overset{T.1.3.6}{=} c_{DIA} \cdot P_{SRC}(t) \qquad \Big/ c_{DIA} \overset{T.1.3.7}{=} \prod_{i=1}^{N} c_i \cdot c_\infty$$

$$\mathcal{S}(t) = \prod_{i=1}^{N} c_i \cdot c_\infty P_{SRC} \qquad \Big/ 2 \text{ arrays, 37 channels } a \in \widehat{2}, j \in \widehat{37}$$

$$\mathcal{S}^{aj}(t) = \prod_{i=1}^{N} c_i^{aj} \cdot c_\infty^{aj} P_{SRC}^{aj} \qquad \Big/ : \mathcal{S}^{aref}(t) = \prod_{i=1}^{N} c_i^{aref} \cdot c_\infty^{aref}$$

$$\frac{\mathcal{S}^{aj}(t)}{\mathcal{S}^{aref}(t)} = \frac{\prod_i c_i^{aj}}{\prod_i c_i^{aref}} \cdot \frac{c_\infty^{aj}}{c_\infty^{aref}} \cdot \frac{P_{SRC}^{aj}}{P_{SRC}^{aref}} \qquad \Big/ \forall a, j, i : P_{SRC}^{aj} = P_{SRC}^{ai}$$

$$\frac{\mathcal{S}^{aj}(t)}{\mathcal{S}^{aref}(t)} = \frac{\prod_i c_i^{aj}}{\prod_i c_i^{aref}} \cdot \frac{c_\infty^{aj}}{c_\infty^{aref}} \qquad \Big/ \forall a \in \widehat{2}, \forall j, k \in \widehat{N-1} c_i^{aj} = c_i^{ak}$$

$$\frac{\mathcal{S}^{aj}(t)}{\mathcal{S}^{aref}(t)} = \frac{c_N^{aj}}{c_N^{aref}} \cdot \frac{c_\infty^{aj}}{c_\infty^{aref}} \qquad \Big/ : \frac{c_N^{aj}}{c_N^{aref}}$$

$$\frac{\mathcal{S}^{aj}(t)}{\mathcal{S}^{aref}(t)} \cdot \frac{c_N^{aref}}{c_N^{aj}} = \frac{c_\infty^{aj}}{c_\infty^{aref}}$$

This relation allows us gain the relative *scalar diagnostics coefficients of unknown*. However, a measured signals $\mathcal{S}$ are required along with some *partial scalar diagnostics coefficients*. For our purposes, we consider only one partial coefficient related to one diagnostics part, the Nth part. Other were considered as the same for all channels. This could be done differently (others parts could be considered too, the $N-1$th too, etc.), but it does not really matter.

The signals $\mathcal{S}^{aj}$ may be gained from following experimental schema, see Fig.2.25. Moreover, the schema (if partial coefficients for optical fibers are approximately the same $\forall j, k \in \widehat{37} : c_{OF}^{j} = c_{OF}^{k}$) also meets

$$\forall a \in \widehat{2} \forall j, k \in \widehat{37} : \qquad c_{SRC}^{j} = c_{SRC}^{k} \qquad c_{PMT}^{j} = c_{PMT}^{k} \qquad c_{OSC}^{j} = c_{OSC}^{k}$$

which represents simple fact: only one light source (SRC), one photomultipler (PMT) and one oscilloscope (OSC) were used during the experiment. Its clear that the same light source produces the same power $P_{SRC}^{aj} = P_{SRC}^{bk}$, which were used in the relationship derivation too. Only observation geometry and optical fibers differ. Well, the optical fibers differences were neglected, so only observation scalar diagnostics coefficients c_{OBS}^{aj} remains.

Normalised signals $\mathcal{S}^{aj}/\mathcal{S}^{aref}$ were measured and plotted in Figs.2.26,2.27. Observation partial scalar diagnostics coefficients were used from T.2.5.7. The final *scalar diagnostics coefficients of unknown* are gained directly from the derived relation and plotted in Figs.2.23,2.24. Q.E.D.

2.5.9 Note

Every diagnostics should have *scalar diagnostics coefficients of unknown* $c_\infty = 1$. This value express that there is no unknown in the diagnostics, all parts are understood theoretically and calibrated

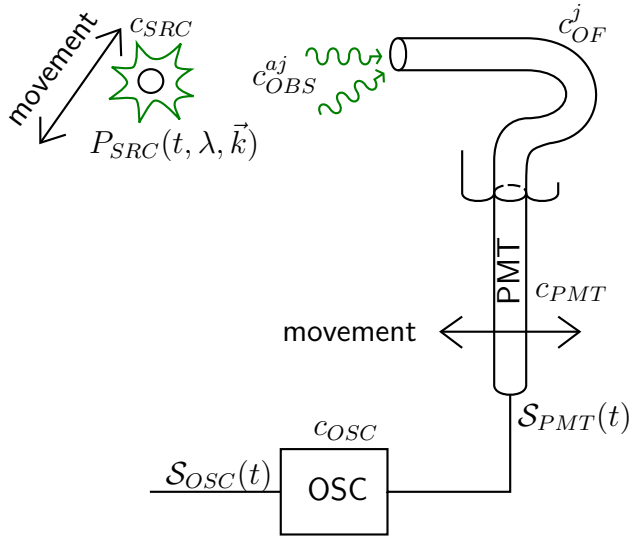

Figure 2.25: Experiment schema for observation *partial scalar diagnostics coefficient* check by estimation of *scalar diagnostics coefficient of unknown*

properly. In practice, the coefficient of unknown may gain various values:

- $c_\infty \approx 1$: most of the diagnostics parts are calibrated well, small deviations are present. Standard deviation is estimated.
- $c_\infty \gg 1 \vee c_\infty \ll 1$: some diagnostics parts are not calibrated well or serious mistakes are present in theory.
- $\forall j,k \in \hat{K} : j \neq k \exists c^j_\infty : c^j_\infty \not\approx c^k_\infty$: diagnostics contains more channels, which unknown differs greatly $\Rightarrow$ dependence on some hidden parameter happens.

It should be also clear that all coefficient approximation may not be valid at all. Thus, all assumtions should be considered carefully before applying the theorem T.1.3.6. If the approximation is not possible, maybe an approximation by a matrix of scalars or matrix of functions should be more appropriate.

The VIS diagnostics results in Figs.2.23.2.24 of relative coefficients of unknown indicate that the approximation is valid enough for core channels. However, the edge channels should require more sophisticated theory understanding. Moreover, the results provide only *relative* coefficients, not the *absolute*. Channels comparision has been done, absolute calibration awaits.

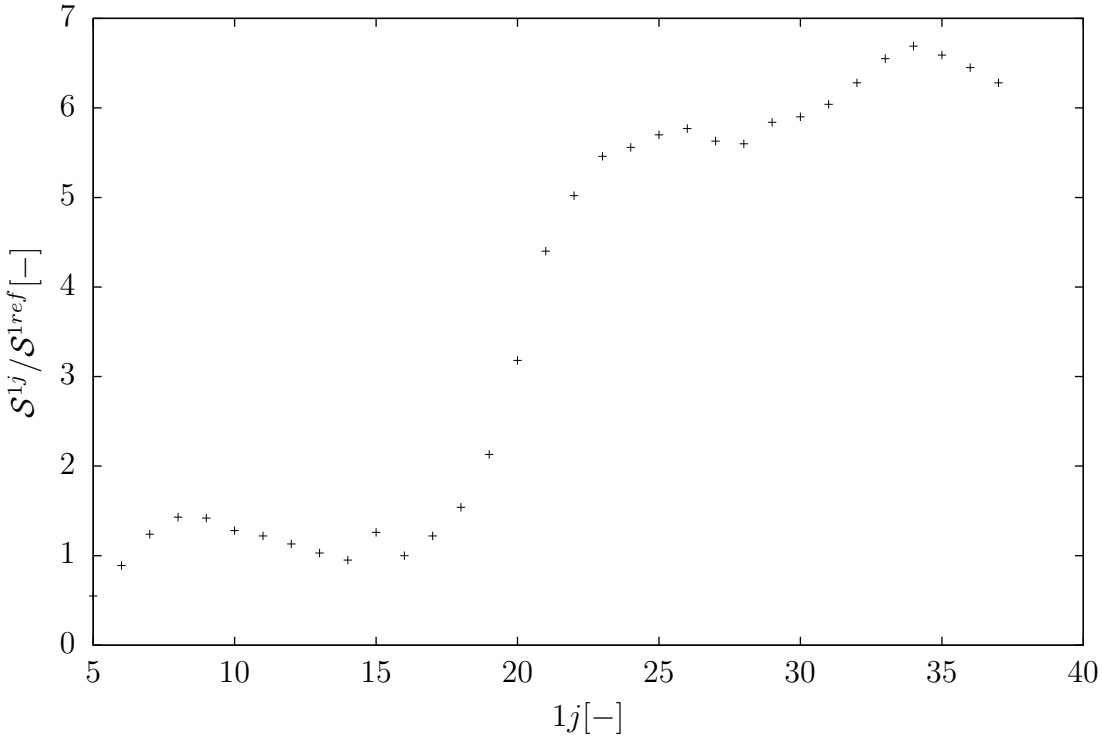

Figure 2.26: VIS TOP normalised measured signal from experiment Fig.2.25. Reference channel was channel No.16

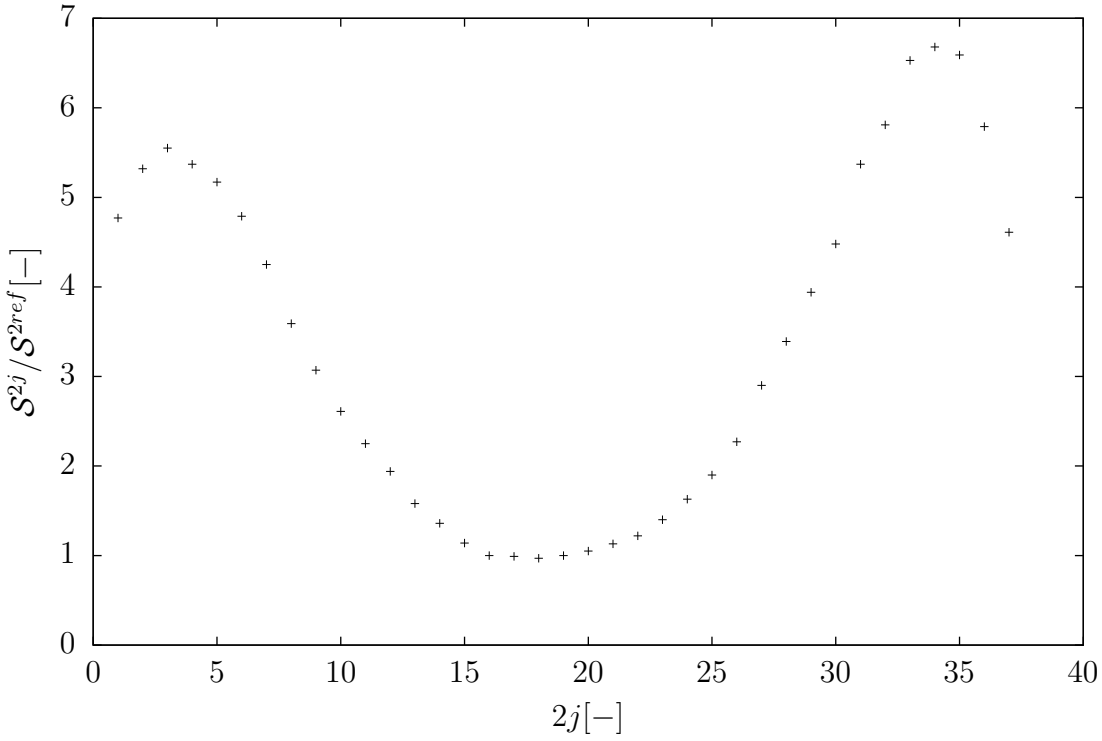

Figure 2.27: VIS BOT normalised measured signal from experiment Fig.2.25. Reference channel was channel No.19

Bibliography

[1] GRIEM, H.R. *Principles of Plasma Spectroscopy*, Cambridge University Press, 2005. ISBN 0-521-61941-6.

[2] WICKERT, M. *ECE 2610 Signal and Systems*, [online]. 2013, [cit. 2013-08-24]. URL: <http://eas.uccs.edu/wickert/ece2610/lecture_notes/ece2610_chap9.pdf >

[3] FRIEDBERG, Jeffry. *Plasma Physics and Fusion Energy*, Cambridge University Press, 2007. ISBN 978-0-511-27375-9.

[4] SEDLÁK, L. *Development of optical diagnostics for the COMPASS tokamak*. 2011. Bachelor thesis at Faculty of Nuclear Sciences and Physical Engineering of Czech Technical University in Prague.

[5] NAYDENKOVA, Diana et al. First spectroscopic measurements on the COMPASS tokamak. In *WDS'09 Proceedings of Contributed Papers: Part II - Physics of Plasmas and Ionized Media*. J. Safrankova, J. Pavlu. Prague: MATFYZPRESS, 2009. P. 158-162. ISBN 978-80-7378-102-6.

[6] ŠESTÁK, D. et at. Design and engineering of optical diagnostic for COMPASS. In *Fusion Engineering and Design 84*. Elsevier, 2009. P. 1755-1758.

[7] NAYDENKOVA, Diana et al. Progress in Multi channel Optical System for Visible Plasma Radiation Measurement at COMPASS Tokamak. In *WDS'10 Proceedings of Contributed Papers: Part II - Physics of Plasmas and Ionized Media*. J. Safrankova, J. Pavlu. Prague: MATFYZPRESS, 2010. P. 18–21. ISBN 978-80-7378-140-8

[8] TKACHENKO, Nikolai V. *Optical Spectroscopy: Methods and Instrumentations*, First edition. Elsevier, 2006. ISBN 978-0-444-52126-2

[9] KUNZE, Hanz-Joachim. *Introduction to Plasma Spectrscopy*. 1th edition. Springer, 2009. ISBN 978-3-642-02232-6

[10] WESSON, J., et al. *Tokamaks*. 3rd edition. Clarendon: Press-Oxford, 2004. ISBN 0-19-8509227.